

Proof of Convergence and Performance Analysis for Sparse Recovery via Zero-point Attracting Projection

Xiaohan Wang, Yuantao Gu, and Laming Chen

Abstract—A recursive algorithm named Zero-point Attracting Projection (ZAP) is proposed recently for sparse signal reconstruction. Compared with the reference algorithms, ZAP demonstrates rather good performance in recovery precision and robustness. However, any theoretical analysis about the mentioned algorithm, even a proof on its convergence, is not available. In this work, a strict proof on the convergence of ZAP is provided and the condition of convergence is put forward. Based on the theoretical analysis, it is further proved that ZAP is non-biased and can approach the sparse solution to any extent, with the proper choice of step-size. Furthermore, the case of inaccurate measurements in noisy scenario is also discussed. It is proved that disturbance power linearly reduces the recovery precision, which is predictable but not preventable. The reconstruction deviation of p -compressible signal is also provided. Finally, numerical simulations are performed to verify the theoretical analysis.

Index Terms—Compressive Sensing (CS), Zero-point Attracting Projection (ZAP), sparse signal reconstruction, ℓ_1 norm, convex optimization, convergence analysis, perturbation analysis, p -compressible signal.

I. INTRODUCTION

A. Overview of CS and Sparse Signal Recovery

Compressive Sensing (CS) [1], [2] is proposed as a novel technique in the field of signal processing. Based on the sparsity of signals in some typical domains, this method takes global measurements instead of samples in signal acquisition. The theory of CS confirms that the measurements required for recovery are far fewer than conventional signal acquisition technique.

With the advantages of sampling below Nyquist rate and little loss in reconstruction quality, CS can be widely applied in the regions such as source coding [3], medical imaging [4], pattern recognition [5], and wireless communication [6].

Suppose that an N -dimensional vector $\mathbf{x} \in \mathbb{R}^N$ is a sparse signal with sparsity S , which means that only S entries of \mathbf{x} are nonzero among all N elements. An $M \times N$ measurement matrix \mathbf{A} with $M < N$ is applied to take global measurements of \mathbf{x} . Consequently an $M \times 1$ vector

$$\mathbf{y} = \mathbf{A}\mathbf{x} \quad (1)$$

is obtained and the information of N -dimensional unknown signal is reduced to the M -dimensional measurement vector.

Xiaohan Wang, Yuantao Gu, and Laming Chen are with the Department of Electronic Engineering, Tsinghua University, Beijing 100084, CHINA. (e-mail: gyt@tsinghua.edu.cn).

This work was partially supported by National Natural Science Foundation of China (NSFC 60872087 and NSFC U0835003).

Exploiting the sparse property of \mathbf{x} , the original signal can be reconstructed through \mathbf{y} and \mathbf{A} .

The procedure of CS mainly includes two stages: signal measurement and signal reconstruction. The key issues are the design of measurement matrix and the algorithm of sparse signal reconstruction, respectively.

On the signal reconstruction of CS, a key problem is to derive the sparse solution, i.e., the solution to the under-determined linear equation which has the minimal ℓ_0 norm,

$$\min_{\mathbf{x}} \|\mathbf{x}\|_0, \quad \text{subject to } \mathbf{y} = \mathbf{A}\mathbf{x}. \quad (P_0)$$

However, (P_0) is a Non-deterministic Polynomial (NP) hard problem. It is demonstrated that under certain conditions [2], (P_0) has the same solution as the relaxed problem

$$\min_{\mathbf{x}} \|\mathbf{x}\|_1, \quad \text{subject to } \mathbf{y} = \mathbf{A}\mathbf{x}. \quad (P_1)$$

(P_1) is a convex problem and can be solved through convex optimization.

In non-ideal scenarios, the measurement vector \mathbf{y} is inaccurate with noise perturbation and (1) never satisfies exactly. Consequently, (P_1) is modified to

$$\min_{\mathbf{x}} \|\mathbf{x}\|_1, \quad \text{subject to } \|\mathbf{y} - \mathbf{A}\mathbf{x}\|_2 \leq \varepsilon, \quad (P_2)$$

where ε is a positive number representing the energy of noise.

Many algorithms have been proposed to recover the sparse signal from \mathbf{y} and \mathbf{A} . These algorithms can be classified into several main categories, including greedy pursuit, optimization algorithms, iterative thresholding algorithms and other algorithms.

The greedy pursuit algorithms always choose the locally optimal approximation to the sparse solution iteratively in each step. The computation complexity is low but more measurements are needed for reconstruction. Typical algorithms include Matching Pursuit (MP) [7], Orthogonal Matching Pursuit (OMP) [8], [9], Stage-wise OMP (StOMP) [10], Regularized OMP (ROMP) [11], [12], Compressive Sampling MP (CoSaMP) [13], Subspace Pursuit (SP) [14], and Iterative Hard Thresholding (IHT) [15].

Optimization algorithms solve convex or non-convex problems and can be further divided into convex optimization and non-convex optimization. Convex optimization methods have the properties of fewer measurements demanded, higher computation complexity, and more theoretical support in mathematics. Convex optimization algorithms include Primal-Dual interior method for Convex Objectives

(PDCO) [16], Least Square QR (LSQR) [17], Large-scale ℓ_1 -regularized Least Squares (ℓ_1 -ls) [18], Least Angle Regression (LARS) [19], Gradient Projection for Sparse Reconstruction (GPSR) [20], Sparse Reconstruction by Separable Approximation (SpARSA) [21], Spectral Projected-Gradient ℓ_1 (SPGL1) [22], Nesterov Algorithm (NESTA) [23] and Constrained Split Augmented Lagrangian Shrinkage Algorithm (C-SALSA) [24].

Non-convex optimization methods solve the problem of optimization by minimizing ℓ_p norm with $0 \leq p < 1$, which is not convex. This category of algorithms demands fewer measurements than convex optimization methods. However, the non-convex property may lead to converging towards the local extremum which is not the desired solution. Moreover, these methods have higher computation complexity. Typical non-convex optimization methods are FOCal Underdetermined System Solver (FOCUSS) [25], Iteratively Reweighted Least Square (IRLS) [26] and ℓ_0 Analysis-based Sparsity (LOAbS) [27].

A new kind of method, Zero-point Attracting Projection (ZAP), has been recently proposed to solve (P_0) or (P_1) [28]. The projection of the zero-point attraction term is utilized to update the iterative solution in the solution space. Compared with the other algorithms, ZAP has advantages of faster convergence rate, fewer measurements demanded, and a better performance against noise.

However, ZAP is proposed with heuristic and experimental methodology and lacks a strict proof of convergence [28]. Though abundant computer simulations verify its performance, it is still essential to prove its convergence, provide the specific working condition, and analyze performances theoretically including the reconstruction precision, the convergence rate and the noise resistance.

B. Our Work

This paper aims to provide a comprehensive analysis for ZAP. Specifically, it studies ℓ_1 -ZAP, which uses the gradient of ℓ_1 norm as the zero-point attraction term.

The main contribution of this work is to prove the convergence of ℓ_1 -ZAP in non-noisy scenario. Our idea is summarized as follows. Firstly, the distance between the iterative solution of ℓ_1 -ZAP and the original sparse signal is defined to evaluate the convergence. Then we prove that such distance will decrease in each iteration, as long as it is larger than a constant proportional to the step-size. Therefore, it is proved that ℓ_1 -ZAP is convergent to the original sparse signal under non-noisy case, which provides a theoretical foundation for the algorithm.

Another contribution is about the signal reconstruction with measurement noise. It is demonstrated that ℓ_1 -ZAP can approach the original sparse signal to some extent under inaccurate measurements. In the noisy case, the recovery precision is linear with not only the step-size but also the energy of noise.

Other contributions include the discussions on some related topics. The convergence rate is estimated as an upper bound of iteration number. The constraint of initial value and its

influence on convergence are provided. The convergence of ℓ_1 -ZAP for p -compressible signal is also discussed. Experiment results are provided to verify the analysis.

The remainder of this paper is organized as follows. In Section II, some preliminary knowledge is introduced to prepare for the main theorems. The main contribution in non-noisy scenario is presented as Theorem 4 in Section III, which proves the convergence of ℓ_1 -ZAP. Some related topics about Theorem 4 are also discussed in Section III. Section IV shows another main theorem in noisy scenario, and some discussions are also brought out. Experiment results are shown in Section V. The whole paper is concluded in Section VI.

II. PRELIMINARIES

A. RIP and Coherence

In this subsection, Restricted Isometry Property (RIP) and coherence are introduced and then some theorems on (P_1) and (P_2) are presented, which will be helpful to the following content.

Definition 1: [29] Suppose $\mathbf{A}_{\mathcal{T}}$ is the $M \times |\mathcal{T}|$ submatrix by extracting the columns of $M \times N$ matrix \mathbf{A} corresponding to the indices in set $\mathcal{T} \subset \{1, 2, \dots, N\}$. The RIP constant δ_S is defined as the smallest nonnegative quantity such that

$$(1 - \delta_S)\|\mathbf{c}\|_2^2 \leq \|\mathbf{A}_{\mathcal{T}}\mathbf{c}\|_2^2 \leq (1 + \delta_S)\|\mathbf{c}\|_2^2$$

holds for all subsets \mathcal{T} with $|\mathcal{T}| \leq S$ and vectors $\mathbf{c} \in \mathbb{R}^{|\mathcal{T}|}$.

Theorem 1: [30] If the RIP constant of matrix \mathbf{A} satisfies the condition

$$\delta_{2S} < \sqrt{2} - 1, \quad (2)$$

where S is the sparsity of \mathbf{x} , then the solution of (P_1) is unique and identical to the original signal.

Theorem 2: [30] If the RIP constant of matrix \mathbf{A} satisfies the condition

$$\delta_{2S} < \sqrt{2} - 1, \quad (3)$$

then the solution \mathbf{x}^* of (P_2) obeys

$$\|\mathbf{x}^* - \mathbf{x}^\sharp\|_2 \leq C_S \varepsilon, \quad (4)$$

where \mathbf{x}^\sharp is the original signal of sparsity S and C_S is a positive constant related to S .

RIP determines the property of the measurement matrix. Recent results on RIP can be found in [31], [32].

Definition 2: [33] The coherence of an $M \times N$ matrix \mathbf{A} is defined as

$$\mu(\mathbf{A}) = \max_{i \neq j} |\alpha_i^T \alpha_j|,$$

where $\alpha_i (1 \leq i \leq N)$ is the i th column of \mathbf{A} and $\|\alpha_i\|_2 = 1$.

Theorem 3: [35], [20] If the sparsity S of \mathbf{x} and the coherence of matrix \mathbf{A} satisfy the condition

$$S < \frac{1}{3\mu(\mathbf{A})}, \quad (5)$$

then the solution of (P_2) is unique.

Theorem 1 provides the sufficient condition on exact recovery of the original signal without any perturbation. It is also a loose sufficient condition of the unique solution of (P_1) . Theorem 2 indicates that under the condition (3), the solution

of (P_2) is not too far from the original signal, with a deviation proportional to the energy of measurement noise. Theorem 3 provides a sufficient condition of the uniqueness of the solution of (P_2) .

B. ℓ_1 -ZAP

In ZAP algorithm, the zero-point attraction term is used to update the iterative solution and then the updated iterative solution is projected to the solution space. The procedures of ZAP can be summarized as follows.

Input: $\mathbf{A} \in \mathbb{R}^{M \times N}$, $\mathbf{y} \in \mathbb{R}^M$, $\gamma \in \mathbb{R}_+$.

Initialization: $n = 0$ and $\mathbf{x}_0 = \mathbf{A}^\dagger \mathbf{y}$.

Iteration:

while stop condition is not satisfied

1. Zero-point attraction:

$$\hat{\mathbf{x}}_{n+1} = \mathbf{x}_n - \gamma \cdot \nabla F(\mathbf{x}_n) \quad (6)$$

2. Projection:

$$\mathbf{x}_{n+1} = \hat{\mathbf{x}}_{n+1} + \mathbf{A}^\dagger (\mathbf{y} - \mathbf{A} \hat{\mathbf{x}}_{n+1}) \quad (7)$$

3. Update the index: $n = n + 1$

end while

In the initialization and (7), $\mathbf{A}^\dagger = \mathbf{A}^T (\mathbf{A} \mathbf{A}^T)^{-1}$ denotes the pseudo-inverse of \mathbf{A} . In (6), $\nabla F(\mathbf{x}_n)$ is the zero-point attraction term, where $F(\mathbf{x})$ is a function representing the sparse penalty of vector \mathbf{x} . Positive parameter γ denotes the step-size in the step of zero-point attraction.

ZAP was firstly proposed in [28] with a specification of ℓ_0 -norm constraint, termed ℓ_0 -ZAP, in which the approximate ℓ_0 norm is utilized as the function $F(\mathbf{x})$. ℓ_0 -ZAP belongs to the non-convex optimization methods and has an outstanding performance beyond conventional algorithms. In [28], the penalty function is $\|\mathbf{x}\|_0$ and its gradient is approximated as

$$\nabla F_{\ell_0}(\mathbf{x}) \approx [f(x_1), f(x_2), \dots, f(x_N)]^T$$

and

$$f(x) = \begin{cases} -\alpha^2 x - \alpha, & -\frac{1}{\alpha} \leq x < 0; \\ -\alpha^2 x + \alpha, & 0 < x \leq \frac{1}{\alpha}; \\ 0, & \text{elsewhere.} \end{cases}$$

The piecewise and non-convex zero-point attraction term further increases the difficulty to theoretically analyze the convergence of ℓ_0 -ZAP.

As another variation of ZAP, ℓ_1 -ZAP is analyzed in this work. The function $F(\mathbf{x})$ is the ℓ_1 norm of \mathbf{x} in the zero-point attraction term. Since it is non-differentiable, the gradient of $F(\mathbf{x})$ can be replaced by its sub-gradient. Considering that the gradient of $F(\mathbf{x})$ is $\text{sgn}(\mathbf{x})$ when none of the components of \mathbf{x} are zero, (6) can be specified as

$$\hat{\mathbf{x}}_{n+1} = \mathbf{x}_n - \gamma \cdot \text{sgn}(\mathbf{x}_n), \quad (8)$$

where the gradient is replaced by one of the sub-gradients $\text{sgn}(\mathbf{x})$. The sign function $\text{sgn}(\mathbf{x})$ has the same size with \mathbf{x} and each entry of $\text{sgn}(\mathbf{x})$ is the scalar sign function of the corresponding entry of \mathbf{x} .

Experiments show that though its performance is better than conventional algorithms, ℓ_1 -ZAP behaves not as good as ℓ_0

norm constraint variation. However, as a convex optimization method, ℓ_1 -ZAP has advantages beyond non-convex methods, as mentioned in introduction. ℓ_1 -ZAP is considered in this paper as the first attempt to analyze ZAP in theory.

The steps (8) and (7) of ℓ_1 -ZAP can be combined into the following recursion

$$\mathbf{x}_{n+1} = \mathbf{x}_n - \gamma \mathbf{P} \text{sgn}(\mathbf{x}_n) \quad (9)$$

with the projection matrix

$$\mathbf{P} = \mathbf{I} - \mathbf{A}^T (\mathbf{A} \mathbf{A}^T)^{-1} \mathbf{A}. \quad (10)$$

Notice that following (9), (10) and the initialization, the sequence has the property

$$\mathbf{A} \mathbf{x}_{n+1} = \mathbf{A} \mathbf{x}_n = \mathbf{A} \mathbf{x}_0 = \mathbf{y}, \quad \forall n \geq 0, \quad (11)$$

which means all iterative solutions fall in the solution space.

Numerical simulations demonstrate that the sparse solution of under-determined linear equation can be calculated by ℓ_1 -ZAP. In fact, the sequence $\{\mathbf{x}_n\}$ calculated through (9) is not strictly convergent. $\{\mathbf{x}_n\}$ will fall into the neighborhood of \mathbf{x}^* after finite iterations, with radius proportional to step-size γ . With the increasing of iterations, \mathbf{x}_n approaches \mathbf{x}^* step by step at first. However, it vibrates in the neighborhood of \mathbf{x}^* when \mathbf{x}_n is close enough to \mathbf{x}^* . If the step-size γ decreases, the radius of neighborhood also decreases. Consequently, one can get the approximation to the sparse solution at any precision by choosing appropriate step-size.

In this work the convergence of ℓ_1 -ZAP is proved. The main results are the following theorems in Section III and IV, corresponding to non-noisy scenario and noisy scenario, respectively.

III. CONVERGENCE IN NON-NOISY SCENARIO

The main contribution is included in this section. A lemma is proposed in Subsection A for preparing the main theorem in Subsection B. Then the condition of exact signal recovery by ℓ_1 -ZAP is given in Subsection C. Several constants and variables in the proof of convergence are discussed in Subsections D and E. In Subsection F, an estimation on the convergence rate is given. The initial value of ℓ_1 -ZAP is discussed in Subsection G.

A. Lemma

Lemma 1: Suppose that $\mathbf{x} \in \mathbb{R}^N$ satisfies $\mathbf{y} = \mathbf{A} \mathbf{x}$, with given $\mathbf{A} \in \mathbb{R}^{M \times N}$ and $\mathbf{y} \in \mathbb{R}^M$. \mathbf{x}^* is the unique solution of (P_1) . If $\|\mathbf{x} - \mathbf{x}^*\|_2$ is bounded by a positive constant M_0 , then there exists a uniform positive constant t depending on \mathbf{A} , \mathbf{y} , and M_0 , such that

$$\|\mathbf{x}\|_1 - \|\mathbf{x}^*\|_1 \geq t \|\mathbf{x} - \mathbf{x}^*\|_2 \quad (12)$$

holds for arbitrary \mathbf{x} satisfying $\mathbf{y} = \mathbf{A} \mathbf{x}$.

The outline of the proof is presented here while the details are included in Appendix A.

Proof: By defining

$$g(\mathbf{x}) = \frac{\|\mathbf{x}\|_1 - \|\mathbf{x}^*\|_1}{\|\mathbf{x} - \mathbf{x}^*\|_2}, \quad (13)$$

equation (12) is equivalent to the following inequality

$$\inf_{\mathbf{x}} g(\mathbf{x}) > 0, \quad \text{subject to } \mathbf{y} = \mathbf{A}\mathbf{x} \text{ and } 0 < \|\mathbf{x} - \mathbf{x}^*\|_2 \leq M_0. \quad (14)$$

Define the index set $\mathcal{I} = \{k \mid x_k^* \neq 0, 1 \leq k \leq N\}$, then there exists a positive constant r_0 such that $(\text{sgn}(\mathbf{x}))_{\mathcal{I}} = (\text{sgn}(\mathbf{x}^*))_{\mathcal{I}}$, when \mathbf{x} satisfies

$$\|\mathbf{x} - \mathbf{x}^*\|_2 < r_0. \quad (15)$$

The above proposition means that \mathbf{x} and \mathbf{x}^* share the same sign for the entries indexed by \mathcal{I} . Consequently, for the separate cases of $0 < \|\mathbf{x} - \mathbf{x}^*\|_2 < r_0$ and $r_0 \leq \|\mathbf{x} - \mathbf{x}^*\|_2 \leq M_0$, it is proved that $g(\mathbf{x})$ has a positive lower bound, respectively. Combining the two cases, Lemma 1 is proved. ■

B. Main Result

Theorem 4: Suppose that \mathbf{x}^* is the unique solution of (P_1) . \mathbf{x}_{n+1} and \mathbf{x}_n satisfies the recursion (9) and \mathbf{x}_n is energy constrained by $\|\mathbf{x}_n - \mathbf{x}^*\|_2 \leq M_0$, where M_0 is a positive constant. Then the iteration obeys

$$\|\mathbf{x}_{n+1} - \mathbf{x}^*\|_2^2 \leq \|\mathbf{x}_n - \mathbf{x}^*\|_2^2 - d\gamma^2 \quad (16)$$

when

$$\|\mathbf{x}_n - \mathbf{x}^*\|_2 \geq K\gamma, \quad (17)$$

where

$$K = \frac{\mu}{2t} \max_{\mathbf{x} \in \mathbb{R}^N} \|\mathbf{P}\text{sgn}(\mathbf{x})\|_2^2, \quad (18)$$

$$d = (\mu - 1) \max_{\mathbf{x} \in \mathbb{R}^N} \|\mathbf{P}\text{sgn}(\mathbf{x})\|_2^2 \quad (19)$$

are two constants with a parameter $\mu > 1$, and $t > 0$ denotes the lower bound specified in Lemma 1.

For a given under-determined constraint (1) and the unique sparsest solution of (P_1) , Theorem 4 demonstrates the convergence property and provides the convergence conditions of ℓ_1 -ZAP. As long as the iterative result \mathbf{x}_n is far away from the sparse solution \mathbf{x}^* , the new result \mathbf{x}_{n+1} in next iteration affirmatively becomes closer than its predecessor. Furthermore, the decrease in ℓ_2 distance is a constant $d\gamma^2$, which means \mathbf{x}_n will definitely get into the $(K\gamma)$ -neighborhood of \mathbf{x}^* in finite iterations. According to the definition of K , \mathbf{x}_n can approach the sparse solution \mathbf{x}^* to any extent if the step-size γ is chosen small enough. Therefore, ℓ_1 -ZAP is convergent, i.e., the iterative result can get close to the sparse solution at any precision. Here μ is a tradeoff parameter which balances the estimated precision and convergence rate.

The proof of Theorem 4 goes in Appendix B.

C. Exact Signal Recovery by ℓ_1 -ZAP

Using Theorem 4 and conditions added, the convergence of ℓ_1 -ZAP can be deduced, as the following corollary.

Corollary 1: Under the condition (2), ℓ_1 -ZAP can recover the original signal at any precision if the step-size γ can be chosen small enough.

Proof: Firstly, it will be demonstrated that the condition of energy constraint in Theorem 4 can always be satisfied. In

fact, M_0 can be chosen greater than $\|\mathbf{x}_0 - \mathbf{x}^*\|_2$. If the energy constraint $\|\mathbf{x}_n - \mathbf{x}^*\|_2 < M_0$ holds for index n , the conditions of Theorem 4 are satisfied and then $\|\mathbf{x}_{n+1} - \mathbf{x}^*\|_2 < M_0$ holds naturally according to (16). Consequently, it is readily accepted that the condition of energy constraint is satisfied for each index n , with the utilization of Theorem 4 in each step.

Combining the explanation after Theorem 4, it is clear that the ℓ_1 -ZAP is convergent to the solution of (P_1) at any precision as long as the step-size is chosen small enough.

According to Theorem 1, it is known that under the condition of (2), the solution of (P_1) is unique and identical to the original sparse signal. Then Corollary 1 is proved. ■

According to Theorem 4 and Corollary 1, the sequence will surely get into the $(K\gamma)$ -neighborhood of \mathbf{x}^* . In fact, because of several inequalities used in the proof, $K\gamma$ is merely a theoretical radius with conservative estimation. The actual convergence may get into a even smaller neighborhood. The details will be discussed in Subsection F.

D. Constant t , K , and the Extremum of $\|\mathbf{P}\text{sgn}(\mathbf{x})\|_2$

Involved in (18) of Theorem 4, constant t is essential to the convergence of ℓ_1 -ZAP. In fact, the key contribution of this work is to indicate the existence of this constant. However, one can merely obtain the existence of t from the proof of Lemma 1, other than its exact value. Because \mathbf{x}^* in the definition of (14) is unknown, it is difficult to give the exact value or formula of t , even though it is actually determined by \mathbf{A} , \mathbf{y} , and M_0 . Whereas, an upper bound is given with some information about t , which leads to Theorem 5.

According to (18), constant K is inversely proportional to t . With a small t , the radius of convergent neighborhood is large and the convergence precision is worse. The maximum of $\|\mathbf{P}\text{sgn}(\mathbf{x})\|_2$ is also involved in the definition of K . According to the range of sign function, i.e. $\{-1, 0, 1\}$, there are 3^N choices of vector $\text{sgn}(\mathbf{x})$ altogether. Similar to t , the extremum of $\|\mathbf{P}\text{sgn}(\mathbf{x})\|_2$ is determined by \mathbf{A} .

The relationship between t and extremum of $\|\mathbf{P}\text{sgn}(\mathbf{x})\|_2$ is presented in Theorem 5.

Theorem 5: If t is defined by (14), one has the following inequality

$$t \leq \min_{\mathbf{x} \in \mathbb{R}^N, \mathbf{x} \neq \mathbf{0}} \|\mathbf{P}\text{sgn}(\mathbf{x})\|_2 \leq \max_{\mathbf{x} \in \mathbb{R}^N} \|\mathbf{P}\text{sgn}(\mathbf{x})\|_2 \leq \sqrt{N}. \quad (20)$$

The proof of Theorem 5 is postponed to Appendix C.

According to the theorem, the minimum of $\|\mathbf{P}\text{sgn}(\mathbf{x})\|_2$ restricts the value of t , as leads to worse precision of ℓ_1 -ZAP. Hence, the measurement matrix \mathbf{A} should be chosen with relatively large $\min \|\mathbf{P}\text{sgn}(\mathbf{x})\|_2$ to improve the performance of the mentioned algorithm. The mathematical meaning of $\mathbf{P}\text{sgn}(\mathbf{x})$ is the projection of $\text{sgn}(\mathbf{x})$ to the solution space of $\mathbf{y} = \mathbf{A}\mathbf{x}$. For a particular instance, if there exists a sign vector, to whom the solution space is almost orthogonal, then the minimum of $\|\mathbf{P}\text{sgn}(\mathbf{x})\|_2$ is rather small and the precision of convergence is bad. An additional explanation is that the solution space can not be strictly orthogonal to any sign vector, or else it will lead to a contradiction with the condition of (2), i.e., the uniqueness of \mathbf{x}^* .

E. Discussions on μ and Bound Sequence

A parameter μ is involved in Theorem 4. We will discuss the choice of μ and some related problems. First of all, it needs to be stressed that μ is just a parameter for the bound sequence in theoretical analysis, other than a parameter for actual iterations.

According to the proof in Appendix B, as long as μ is chosen satisfying the conditions of $\mu > 1$ and

$$\|\mathbf{x}_n - \mathbf{x}^*\|_2 \geq \gamma \frac{\mu}{2t} \max_{\mathbf{x} \in \mathbb{R}^N} \|\mathbf{P}\text{sgn}(\mathbf{x})\|_2^2,$$

Theorem 4 holds and the distance between \mathbf{x}_n and \mathbf{x}^* decreases in the next iteration. However, considering the expression of (19), the decrease of $\|\mathbf{x}_n - \mathbf{x}^*\|_2^2$ by each iteration is different for various μ . There are two strategies to choose the parameter μ , a constant or a variable one.

When μ is chosen as a constant, Theorem 4 indicates that as long as the distance between \mathbf{x}_n and \mathbf{x}^* is larger than $K\gamma$, the next iteration leads to a decrease at least a constant step of $d\gamma^2$.

When the parameter μ is variable, the decrease step of $\|\mathbf{x}_n - \mathbf{x}^*\|_2$ is also variable. The expressions show that K and d increase as the increase of μ . Notice that μ must obey

$$1 < \mu \leq \frac{2t}{\gamma} \frac{\|\mathbf{x}_n - \mathbf{x}^*\|_2}{\max_{\mathbf{x} \in \mathbb{R}^N} \|\mathbf{P}\text{sgn}(\mathbf{x})\|_2^2}, \quad (21)$$

where the right inequality is necessary to satisfy (17), which ensures the convergence of the sequence. During the very beginning of recursions, \mathbf{x}_n is far from \mathbf{x}^* . Consequently, μ satisfying (21) can be larger, and lead to a faster convergence. However, as \mathbf{x}_n gets closer to \mathbf{x}^* by iterations, μ satisfying (21) is definitely just a little larger than one.

To be emphasized, the actual convergence of iterations can not speed up by choosing the parameter μ . The value of μ only impacts the sequence of

$$\|\mathbf{x}'_{n+1} - \mathbf{x}^*\|_2^2 = \|\mathbf{x}'_n - \mathbf{x}^*\|_2^2 - d\gamma^2, \quad (22)$$

which is a sequence bounding the actual sequence in the proof of convergence.

F. Convergence Rate

Theorem 4 tells little about the convergence rate. Considering several inequalities utilized in the proof, the actual convergence is faster than that of the sequence in (22). It means that a lower bound of the convergence rate can be derived in theory.

Corresponding to the variable selection of μ , a sequence $\{\mathbf{x}'_n\}$ is put forward with properties

$$\|\mathbf{x}'_{n+1} - \mathbf{x}^*\|_2^2 = \|\mathbf{x}'_n - \mathbf{x}^*\|_2^2 - \gamma^2(\mu_n - 1) \max_{\mathbf{x} \in \mathbb{R}^N} \|\mathbf{P}\text{sgn}(\mathbf{x})\|_2^2, \quad (23)$$

where

$$\mu_n = \frac{2t\|\mathbf{x}'_n - \mathbf{x}^*\|_2}{\gamma \max_{\mathbf{x} \in \mathbb{R}^N} \|\mathbf{P}\text{sgn}(\mathbf{x})\|_2^2} > 1. \quad (24)$$

Combining (23) and (24), the iteration of \mathbf{x}'_n obeys

$$\begin{aligned} \|\mathbf{x}'_{n+1} - \mathbf{x}^*\|_2^2 &= \|\mathbf{x}'_n - \mathbf{x}^*\|_2^2 - 2\gamma t \|\mathbf{x}'_n - \mathbf{x}^*\|_2 \\ &\quad + \gamma^2 \max_{\mathbf{x} \in \mathbb{R}^N} \|\mathbf{P}\text{sgn}(\mathbf{x})\|_2^2. \end{aligned} \quad (25)$$

The distance between \mathbf{x}'_n and \mathbf{x}^* with variable μ decreases the most for each step. Therefore, $\{\mathbf{x}'_n\}$ has a faster convergence rate compared with sequences satisfying (22) with other choices of μ . However, as a theoretical result, it still converges more slowly than the actual sequence.

Derived from Lemma 2, which gives a rough estimation, Theorem 6 provides a much better lower bound of the convergence rate.

Lemma 2: Supposing $\{\mathbf{x}_n\}$ is the iterative sequence by ℓ_1 -ZAP, it will take at most

$$\frac{2(K_{\max} - K_{\min})}{2t - \max_{\mathbf{x} \in \mathbb{R}^N} \|\mathbf{P}\text{sgn}(\mathbf{x})\|_2^2 / K_{\min}}$$

steps for $\{\mathbf{x}_n\}$ to get into the $(K_{\min}\gamma)$ -neighborhood from the $(K_{\max}\gamma)$ -neighborhood of \mathbf{x}^* , where $K_{\max} > K_{\min}$ and K_{\min} must obey

$$K_{\min} > \frac{1}{2t} \max_{\mathbf{x} \in \mathbb{R}^N} \|\mathbf{P}\text{sgn}(\mathbf{x})\|_2^2. \quad (26)$$

Theorem 6: Supposing $\{\mathbf{x}_n\}$ is the iterative sequence by ℓ_1 -ZAP, it will get into the $(K_0\gamma)$ -neighborhood of \mathbf{x}^* within at most

$$\frac{M_0}{t\gamma} + \frac{K_0}{t} \ln \left(\frac{M_0}{K_0\gamma} \right) + \frac{2K_0}{2t - \max_{\mathbf{x} \in \mathbb{R}^N} \|\mathbf{P}\text{sgn}(\mathbf{x})\|_2^2 / K_0}$$

steps. Here M_0 , γ , and t have the same definitions with those in Theorem 4, and K_0 must obey

$$K_0 > \frac{1}{2t} \max_{\mathbf{x} \in \mathbb{R}^N} \|\mathbf{P}\text{sgn}(\mathbf{x})\|_2^2.$$

The proofs of Lemma 2 and Theorem 6 are postponed to Appendix D and E, respectively.

G. Choice of the Initial Value

In ℓ_1 -ZAP, the initial value is the least square solution of the under-determined equation,

$$\mathbf{x}_0 = \mathbf{A}^T(\mathbf{A}\mathbf{A}^T)^{-1}\mathbf{y}.$$

From Theorem 4 and Corollary 1, one knows that if the initial value obeys $\mathbf{A}\mathbf{x}_0 = \mathbf{y}$, the iterative sequence $\{\mathbf{x}_n\}$ is convergent. Therefore, the restriction to the initial value is to be in the solution space, other than to be the least square solution. However, it is still a convenient way to initialize using the least square solution.

IV. CONVERGENCE IN NOISY SCENARIO

The convergence of ℓ_1 -ZAP in noisy scenario is analyzed in this section. The main theorem in noisy scenario is given in Subsection A. In Subsection B, the problem of signal recovery from inaccurate measurements is discussed. Subsection C shows different choices of initial value and the impact on the quality of reconstruction. The reconstruction of p -compressible signal by ℓ_1 -ZAP is discussed in Subsection D.

A. Main Result in Noisy Scenario

Considering the perturbation on measurement vector \mathbf{y} , Theorem 7 is presented to analyze the convergence of ℓ_1 -ZAP. Similar to Lemma 1, Lemma 3 is proposed at first corresponding to the noisy case.

Lemma 3: Suppose that $\mathbf{x} \in \mathbb{R}^N$ satisfies $\|\mathbf{y} - \mathbf{A}\mathbf{x}\|_2 \leq \varepsilon$, with given $\mathbf{A} \in \mathbb{R}^{M \times N}$ and $\mathbf{y} \in \mathbb{R}^M$. \mathbf{x}^* is the unique solution of (P_2) . $\|\mathbf{x} - \mathbf{x}^*\|_2$ is bounded by a positive number M_0 . Then there exists a positive number t depending on \mathbf{A} , \mathbf{y} , M_0 , and ε , such that

$$\|\mathbf{x}\|_1 - \|\mathbf{x}^*\|_1 \geq t\|\mathbf{x} - \mathbf{x}^*\|_2. \quad (27)$$

Proof: With the definition of (13), (27) is equivalent to the following inequality

$$\inf_{\mathbf{x}} g(\mathbf{x}) > 0, \quad \text{subject to } \|\mathbf{y} - \mathbf{A}\mathbf{x}\|_2 \leq \varepsilon \text{ and } 0 < \|\mathbf{x} - \mathbf{x}^*\|_2 \leq M_0. \quad (28)$$

Following the proof of Lemma 1, it can be readily proved that Lemma 3 is correct. Notice that here

$$\mathbf{u} = \frac{\mathbf{x} - \mathbf{x}^*}{\|\mathbf{x} - \mathbf{x}^*\|_2}$$

is not in the null-space of \mathbf{A} , but a unit vector satisfying $\|\mathbf{A}\mathbf{u}\|_2 \leq 2\varepsilon$. The remaining procedures are similar. The details of the proof are omitted for short. ■

Theorem 7: Supposing that \mathbf{x}^* is the unique solution of (P_2) , sequence $\{\mathbf{x}_n\}$ satisfies the iterative formula (9) with conditions

$$\|\mathbf{y} - \mathbf{A}\mathbf{x}_n\|_2 \leq \varepsilon \quad (29)$$

and

$$\|\mathbf{x}_n - \mathbf{x}^*\|_2 \leq M_0, \quad (30)$$

where M_0 is a positive constant. Then the iteration obeys

$$\|\mathbf{x}_{n+1} - \mathbf{x}^*\|_2^2 \leq \|\mathbf{x}_n - \mathbf{x}^*\|_2^2 - d\gamma^2,$$

when

$$\|\mathbf{x}_n - \mathbf{x}^*\|_2 \geq K\gamma + C\varepsilon,$$

where $C = 2\sqrt{N\lambda}/t$, K and d are defined by (18) and (19), respectively. Here $\mu > 1$ is a parameter, t is the positive lower bound in Lemma 3, and λ is the largest eigenvalue of matrix $(\mathbf{A}\mathbf{A}^T)^{-1}$.

The proof of Theorem 7 goes in Appendix F.

Theorem 7 indicates that under measurement perturbation with energy less than ε , the iterative sequence $\{\mathbf{x}_n\}$ will get into the $(K\gamma + C\varepsilon)$ -neighborhood of \mathbf{x}^* . For the fixed original signal and measurement matrix, the precision of \mathbf{x}_n approaching \mathbf{x}^* depends on both the step-size and the noise energy bound. It means that \mathbf{x}_n can not get close to the solution \mathbf{x}^* at any precision by choosing small step-size, because the noise energy also controls a deviation component, $C\varepsilon$.

B. Signal Recovery from Inaccurate Measurements

Corollary 2 indicates the property of signal reconstruction with inaccurate measurements.

Corollary 2: Suppose the original signal is $\mathbf{x}^\sharp \in \mathbb{R}^N$, and the conditions of (3) and (5) are satisfied. There exist real numbers $K > 0$, $C' > 0$ such that ℓ_1 -ZAP can be convergent to a $(K\gamma + C'\varepsilon)$ -neighborhood of \mathbf{x}^\sharp , i.e., ℓ_1 -ZAP can approach the original signal to some extent under inaccurate measurements.

Proof: Referring to the proof of Corollary 1, it can be readily accepted that the condition (30) is always satisfied for any index n . It is known from Theorem 3 that (P_2) has a unique solution under the condition (5). Consequently, according to Theorem 7, the sequence $\{\mathbf{x}_n\}$ finally gets into the neighborhood of \mathbf{x}^* with the radius $K\gamma + C\varepsilon$.

Theorem 2 shows that under the condition of (3), the solution of (P_2) is not far from the original signal \mathbf{x}^\sharp , with the inequality

$$\|\mathbf{x}^* - \mathbf{x}^\sharp\|_2 \leq C_S\varepsilon. \quad (31)$$

Combining Theorem 7, (31), and the triangle inequality, one sees that the sequence gets into the neighborhood of \mathbf{x}^\sharp with the radius $K\gamma + (C + C_S)\varepsilon$. Denote $C' = C + C_S$ and the conclusion of Corollary 2 is drawn. ■

C. Initial Values

Among the assumptions of Theorem 7, a condition of (29) is assumed to be satisfied. Considering the recursion (9), one readily sees that

$$\|\mathbf{y} - \mathbf{A}\mathbf{x}_n\|_2 = \|\mathbf{y} - \mathbf{A}\mathbf{x}_0\|_2. \quad (32)$$

Under the simple condition of

$$\|\mathbf{y} - \mathbf{A}\mathbf{x}_0\|_2 \leq \varepsilon, \quad (33)$$

where \mathbf{x}_0 is not necessarily the least square solution of $\mathbf{y} = \mathbf{A}\mathbf{x}$, it will suffice to get (29), which satisfies the condition of Theorem 7.

If the initial value satisfies (33), by defining $\mathbf{e}_n = \mathbf{A}(\mathbf{x}_n - \mathbf{x}^*)$, one has

$$\begin{aligned} \|\mathbf{e}_n\|_2 &= \|(\mathbf{y} - \mathbf{A}\mathbf{x}_n) - (\mathbf{y} - \mathbf{A}\mathbf{x}^*)\|_2 \\ &\leq \|\mathbf{y} - \mathbf{A}\mathbf{x}_n\|_2 + \|\mathbf{y} - \mathbf{A}\mathbf{x}^*\|_2 \leq 2\varepsilon. \end{aligned} \quad (34)$$

Inequality (34) provides the upper bound of $\|\mathbf{e}_n\|_2$ and it is used to prove Theorem 7.

If the iterations begin with the least square solution of the perturbed measurement \mathbf{y} , it obeys $\mathbf{y} = \mathbf{A}\mathbf{x}_0$ and according to (32) one has

$$\|\mathbf{y} - \mathbf{A}\mathbf{x}_n\|_2 = 0,$$

which means that (34) can be modified to

$$\|\mathbf{e}_n\|_2 \leq \varepsilon. \quad (35)$$

Hence, the parameter ε can be reduced to a half throughout the proof of Theorem 7. Therefore, if the initial value is chosen as the least square solution, the neighborhood of convergence will be smaller, i.e., a better estimation can be reached.

D. Discussions on p -compressible Signal

The original signal is not always absolutely sparse. The reconstruction of compressible signal is discussed here. Signal \mathbf{x} is p -compressible with magnitude R if the components of \mathbf{x} decay as

$$|x_{(i)}| \leq R \cdot i^{-1/p},$$

where $x_{(i)}$ is the i th largest absolute value among the components of \mathbf{x} , and p is a number between 0 and 1. Supposing that \mathbf{x}_S is a best S -sparse approximation to \mathbf{x} , the following inequalities hold [34],

$$\|\mathbf{x} - \mathbf{x}_S\|_1 \leq C_p \cdot R \cdot S^{1-1/p}, \quad (36)$$

$$\|\mathbf{x} - \mathbf{x}_S\|_2 \leq D_p \cdot R \cdot S^{1/2-1/p}, \quad (37)$$

where $C_p = (1/p - 1)^{-1}$ and $D_p = (2/p - 1)^{-1/2}$.

For a p -compressible signal \mathbf{x} , one has

$$\mathbf{y} = \mathbf{A}\mathbf{x} + \mathbf{e} = \mathbf{A}\mathbf{x}_S + (\mathbf{A}(\mathbf{x} - \mathbf{x}_S) + \mathbf{e}).$$

By Proposition 3.5 in [13], the norm of $\mathbf{A}(\mathbf{x} - \mathbf{x}_S)$ can be estimated as

$$\|\mathbf{A}(\mathbf{x} - \mathbf{x}_S)\|_2 \leq \sqrt{1 + \delta_S} \left(\|\mathbf{x} - \mathbf{x}_S\|_2 + \frac{1}{\sqrt{S}} \|\mathbf{x} - \mathbf{x}_S\|_1 \right). \quad (38)$$

Combining (36), (37) and (38), one has

$$\|\mathbf{A}(\mathbf{x} - \mathbf{x}_S) + \mathbf{e}\|_2 \leq \sqrt{1 + \delta_S} (D_p + C_p) \cdot R \cdot S^{1/2-1/p} + \varepsilon.$$

According to Theorem 7 and Corollary 2, the reconstruction property of p -compressible signal by ℓ_1 -ZAP can be deduced as follows.

Corollary 3: Supposing $\mathbf{x} \in \mathbb{R}^N$ is p -compressible signal and the conditions of (3) and (5) are satisfied, then the ℓ_1 -ZAP sequence can approach \mathbf{x} with a deviation

$$K\gamma + C'\varepsilon + C'\sqrt{1 + \delta_S} (D_p + C_p) \cdot R \cdot S^{1/2-1/p},$$

where K and C' are the same with those in Corollary 2, and ε is the energy bound of observation noise.

The non-noisy scenario for compressible signal can be naturally obtained by setting ε to zero in Corollary 3.

V. EXPERIMENTS

Several experiments are conducted in this section. The performance of ℓ_0 -ZAP and ℓ_1 -ZAP are shown in Subsection A, compared with several other algorithms for sparse recovery. The deviations of actual ℓ_1 -ZAP sequence and bound sequences in the proof are illustrated in Subsection B. In Subsection C, experiment results demonstrate the impacts of the step-size and the noise level on the signal reconstruction via ℓ_1 -ZAP.

A. Performance of ZAP

The performances of ℓ_1 -ZAP and ℓ_0 -ZAP are simulated, compared with other sparse recovery algorithms.

In the experiments, the $M \times N$ matrix \mathbf{A} is generated with the entries independent and following a normal distribution with mean zero and variance $1/M$. The support set of original signal \mathbf{x}^* is chosen randomly following uniform distribution.

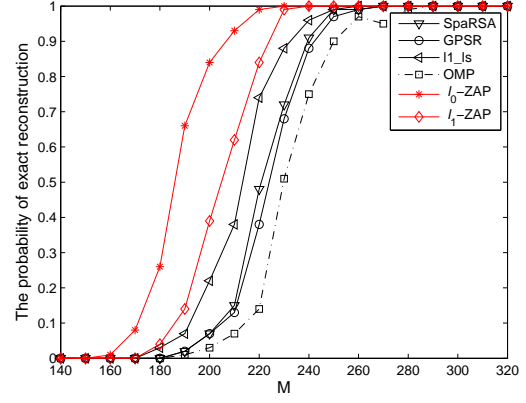


Fig. 1. Probability of exact reconstruction for various number of measurements, where $N = 1000$, $S = 50$.

The nonzero entries follow a normal distribution with mean zero. Finally the energy of the original signal is normalized.

For parameters $N = 1000$, $S = 50$, the probability of exact reconstruction for various number of measurements is shown as Fig. 1. If the reconstruction SNR is higher than a threshold of 40dB, the trial is regarded as exact reconstruction. The number of M varies from 140 to 320 and each point in the experiment is repeated 200 times. The step-size of ℓ_1 -ZAP is 5×10^{-4} . The parameters of other algorithms are selected as recommended by respective authors. It can be seen that for any fixed M from 180 to 260, ℓ_0 -ZAP and ℓ_1 -ZAP have higher probability of reconstruction than other algorithms, which means ZAP algorithms demand fewer measurements in signal reconstructions. The experiment also indicates that the performance of ℓ_0 -ZAP is better than ℓ_1 -ZAP, as discussed in Section II.

For parameters $N = 1000$, $M = 200$, Fig. 2 illustrates the probability of exact reconstruction for various sparsity S from 25 to 70. All the algorithms are repeated 200 times for each value. The parameters of algorithms are the same as those in the previous experiment. ℓ_0 -ZAP has the highest probability for fixed sparsity S and ℓ_1 -ZAP is the second beyond other conventional algorithms. The experiment indicates that ZAP algorithms can recover less sparse signals compared with other algorithms.

The SNR performance is illustrated in Fig. 3 with the measurement SNR varying from 5dB to 30dB and 200 times repeated for each value. The noise is zero-mean white Gaussian and added to the observed vector \mathbf{y} . The parameters are selected as $N = 1000$, $M = 200$ and $S = 30$. The parameters of algorithms have the same choice with previous experiments. The reconstruction SNR and measurement SNR are the signal-to-noise ratios of reconstructed signal $\hat{\mathbf{x}}$ and measurement signal \mathbf{y} , respectively. ℓ_0 -ZAP outperforms other algorithms, while ℓ_1 -ZAP is almost the same as others. The experiment indicates that ℓ_0 -ZAP has a better performance against noise and ℓ_1 -ZAP does not have visible defects compared with other algorithms.

The experiments above demonstrate that ℓ_1 -ZAP has a better performance compared with conventional algorithms.

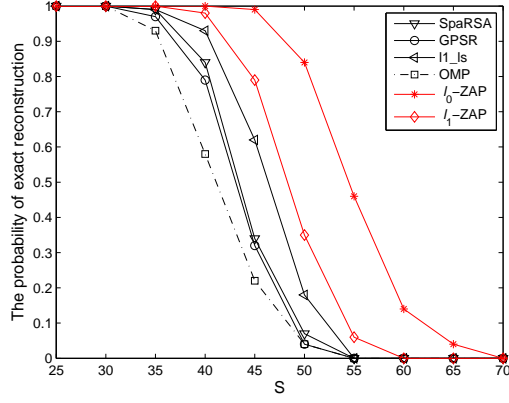


Fig. 2. Probability of exact reconstruction for various sparsity, where $N = 1000$, $M = 200$.

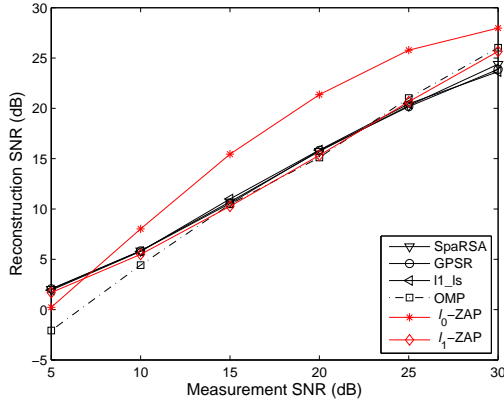


Fig. 3. Reconstruction SNR versus measurement SNR, where $N = 1000$, $M = 200$, $S = 30$.

ℓ_1 -ZAP demands fewer measurements and can recover signals with higher sparsity, with similar property against noise. The performance of ℓ_0 -ZAP is better than ℓ_1 -ZAP.

B. Actual Sequence and Bound Sequences

According to Theorem 4, the deviation from the actual iterative sequence to the sparse solution is bounded by the sequence satisfying (22). In Theorem 4, a sequence with parameter μ is utilized to bound the actual sequence and proved to be convergent. As discussed in III-E and F, the sequence defined in (23) and (24) with adaptive μ approaches the sparse solution faster than any sequence with constant μ .

The reconstruction SNR curves of the actual sequence and three bound sequences with different choices of μ are demonstrated in Fig. 4. As can be seen in the figure, the bound sequence with adaptive μ is the best estimation among different choices. For a constant μ , the larger one leads to faster convergence and less precision.

For adaptive μ , as illustrated in Fig. 4, the reconstruction SNR reaches steady-state after about 2000 iterations. However, referring to Fig. 5, the value of μ keeps decreasing until over 6000 iterations, though it impacts little to the convergence

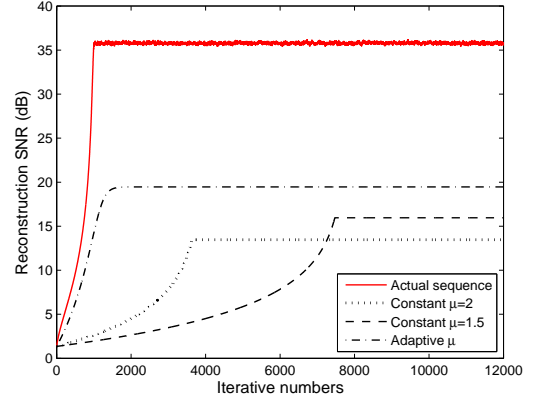


Fig. 4. Reconstruction SNR of actual sequence and bound sequences with different choices of μ , where $M = 250$, $N = 1000$, $S = 50$, $\gamma = 5 \times 10^{-4}$.

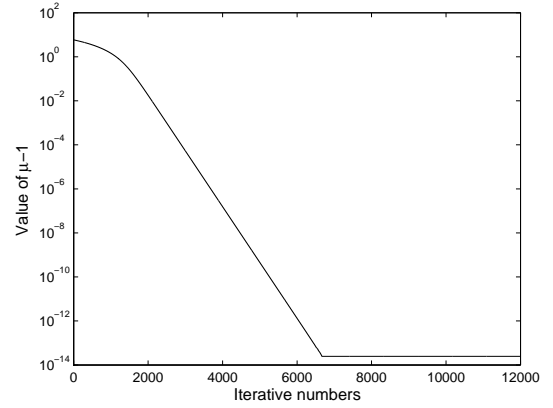


Fig. 5. The value of $\mu - 1$ throughout the iteration for adaptive μ .

behavior. In fact, adaptive μ will decrease towards 1 throughout the iteration and never stop. Nevertheless, the precision of simulation platform limits its variation after it is below 3×10^{-14} .

The deviations of the actual iterative sequence and a bound sequence are both proportional to the step-size, with the difference in the scale factor. Though the bound is not very strict, it does well in the proof of the convergence of ℓ_1 -ZAP.

C. About Step-size and Noise

As proved in Theorem 4, in non-noisy scenario, ℓ_1 -ZAP can reconstruct the original signal at arbitrary precision by choosing the step-size small enough. Theorem 7 demonstrates that in noisy scenario the reconstruction SNR is determined by both the step-size and noise level. Experiment results shown in Fig. 6 verify the analysis. Each combination of step-size and measurement SNR is simulated 100 times. Experiment results indicate that in non-noisy scenario, the reconstruction SNR increases as the decreasing of step-size. In noisy scenario, the reconstruction SNR can not increase arbitrarily due to the impact of noise. For small step-size, the reconstruction SNR is mainly determined by noise level. The reconstruction SNR is higher when the measurement SNR is higher. For large step-

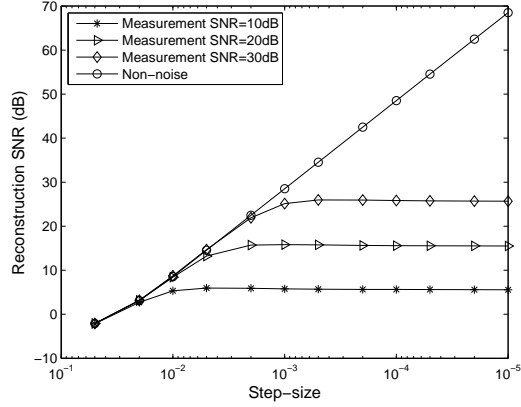


Fig. 6. Reconstruction SNR versus step-size for various SNR, where $M = 150$, $N = 1000$, $S = 20$.

size, the step-size mainly controls the reconstruction SNR and the reconstruction SNR increase as the decreasing of step-size.

The figure also offers a way to choose the step-size under noise. It is not necessary to choose the step-size too small because it benefits little under the impact of noise. For an estimated reconstruction SNR, the best choice of step-size is the value just entered the flat region.

VI. CONCLUSION

This paper provides ℓ_1 -ZAP a comprehensive theoretical analysis. Firstly, the mentioned algorithm is proved to be convergent to a neighborhood of the sparse solution with the radius proportional to the step-size of iteration. Therefore, it is non-biased and can approach the sparse solution to any extent and reconstruct the original signal exactly. Secondly, when the measurements are inaccurate with noise perturbation, ℓ_1 -ZAP can also approach the sparse solution and the precision is linearly reduced by the disturbance power. In addition, some related topics about the initial value and the convergence rate are also discussed. The convergence property of p -compressible signal by ℓ_1 -ZAP is also discussed. Finally, experiments are conducted to verify the theoretical analysis on the convergence process and illustrate the impacts of parameters on the reconstruction results.

VII. APPENDIX

A. The Proof of Lemma 1

Proof: It is to be proved that $g(\mathbf{x})$ defined in (13) has a positive lower bound respectively for $0 < \|\mathbf{x} - \mathbf{x}^*\|_2 < r_0$ and $r_0 \leq \|\mathbf{x} - \mathbf{x}^*\|_2 \leq M_0$, where r_0 is defined in (15).

Define sets \mathcal{X}_1 and \mathcal{X}_2 as

$$\begin{aligned} \mathcal{X}_1 &= \{\mathbf{x} \mid r_0 \leq \|\mathbf{x} - \mathbf{x}^*\|_2 \leq M_0\} \cap \{\mathbf{x} \mid \mathbf{y} = \mathbf{A}\mathbf{x}\}, \\ \mathcal{X}_2 &= \{\mathbf{x} \mid 0 < \|\mathbf{x} - \mathbf{x}^*\|_2 < r_0\} \cap \{\mathbf{x} \mid \mathbf{y} = \mathbf{A}\mathbf{x}\}. \end{aligned} \quad (39)$$

For $\mathbf{x} \in \mathcal{X}_1$, the function $g(\mathbf{x})$ is continuous for \mathbf{x} and the domain is a bounded closed set. As a basic theorem in calculus, the value of a continuous function can reach the infimum if the domain is a bounded closed set. As a consequence, there exists an $\mathbf{x}_0 \in \mathcal{X}_1$, such that $g(\mathbf{x}_0) = \inf_{\mathcal{X}_1} g(\mathbf{x})$. By the

uniqueness of \mathbf{x}^* and the definition of $g(\mathbf{x})$, $g(\mathbf{x})$ is positive in \mathcal{X}_1 . Then $g(\mathbf{x}_0)$ is positive and this leads to the conclusion that the infimum of $g(\mathbf{x})$ is positive in \mathcal{X}_1 .

On the other hand, it will be proved that $g(\mathbf{x})$ has a positive lower bound for $\mathbf{x} \in \mathcal{X}_2$.

Any vector in the solution space of $\mathbf{y} = \mathbf{A}\mathbf{x}^*$ can be represented by

$$\mathbf{x} = \mathbf{x}^* + r \cdot \mathbf{u} \quad (40)$$

where

$$r = \|\mathbf{x} - \mathbf{x}^*\|_2, \quad (41)$$

$$\mathbf{u} = (\mathbf{x} - \mathbf{x}^*) / \|\mathbf{x} - \mathbf{x}^*\|_2 \quad (42)$$

denote the distance and direction, respectively. Considering the definition of r_0 , one has

$$(\mathbf{x}^*)^T \text{sgn}(\mathbf{x}) = (\mathbf{x}^*)^T \text{sgn}(\mathbf{x}^*) = \|\mathbf{x}^*\|_1. \quad (43)$$

Combining (40) with (43), one gets

$$\|\mathbf{x}\|_1 = (\mathbf{x}^* + r \cdot \mathbf{u})^T \text{sgn}(\mathbf{x}) = \|\mathbf{x}^*\|_1 + r \cdot \mathbf{u}^T \text{sgn}(\mathbf{x}). \quad (44)$$

As a consequence, for $0 < r < r_0$, the objective function can be simplified as

$$g(\mathbf{x}) = \frac{\|\mathbf{x}\|_1 - \|\mathbf{x}^*\|_1}{\|\mathbf{x} - \mathbf{x}^*\|_2} = \mathbf{u}^T \text{sgn}(\mathbf{x}) = \sum_{k=1}^N u_k \text{sgn}(x_k). \quad (45)$$

Index set $\mathcal{I} = \{k \mid x_k^* \neq 0, 1 \leq k \leq N\}$ is the support set of \mathbf{x}^* . \mathcal{I}^c denotes the complement of \mathcal{I} . For $\forall k \in \mathcal{I}$, considering the definition of r_0 ,

$$u_k \text{sgn}(x_k) = u_k \text{sgn}(x_k^*).$$

For $\forall k \in \mathcal{I}^c$, considering $x_k^* = 0$ and the definition of \mathbf{u} in (42),

$$u_k \text{sgn}(x_k) = u_k \text{sgn}(u_k) = |u_k|.$$

Consequently, $g(\mathbf{x})$ can be rewritten as a function of \mathbf{u} ,

$$\begin{aligned} g(\mathbf{x}) &= \sum_{k \in \mathcal{I}} u_k \text{sgn}(x_k) + \sum_{k \in \mathcal{I}^c} u_k \text{sgn}(x_k) \\ &= \mathbf{u}_{\mathcal{I}}^T \text{sgn}(\mathbf{x}^*) + \|\mathbf{u}_{\mathcal{I}^c}\|_1 \triangleq G(\mathbf{u}), \end{aligned} \quad (46)$$

where

$$(\mathbf{u}_{\mathcal{I}})_{\mathbf{k}} = \begin{cases} u_k, & k \in \mathcal{I}; \\ 0, & \text{elsewhere,} \end{cases}$$

and

$$\mathbf{u}_{\mathcal{I}^c} = \mathbf{u} - \mathbf{u}_{\mathcal{I}}.$$

It can be seen that $G(\mathbf{u})$ is continuous for \mathbf{u} and the domain of $G(\mathbf{u})$ is $\{\mathbf{u} \in \mathbb{R}^N \mid \|\mathbf{u}\|_2 = 1\} \cap \{\mathbf{u} \in \mathbb{R}^N \mid \mathbf{A}\mathbf{u} = 0\}$. Since the domain of $G(\mathbf{u})$ is the intersection of two closed sets and the first set is bounded, it is a bounded closed set and $G(\mathbf{u})$ can reach the infimum. Then $g(\mathbf{x})$ has the minimum. By the uniqueness of \mathbf{x}^* , $g(\mathbf{x})$ is positive, consequently $\inf_{\mathcal{X}_2} g(\mathbf{x}) > 0$.

To sum up, the lower bound of $g(\mathbf{x})$ is positive for

$$\mathbf{x} \in \mathcal{X}_1 \cup \mathcal{X}_2 = \{\mathbf{x} \mid 0 < \|\mathbf{x} - \mathbf{x}^*\|_2 \leq M_0\} \cap \{\mathbf{x} \mid \mathbf{y} = \mathbf{A}\mathbf{x}\},$$

which completes the proof of Lemma 1. \blacksquare

B. The Proof of Theorem 4

Proof: By denoting

$$\mathbf{h}_n = \mathbf{x}_n - \mathbf{x}^*$$

as the iterative deviation and subtracting the unique solution \mathbf{x}^* from both sides of (9), one has

$$\begin{aligned} & \|\mathbf{h}_{n+1}\|_2^2 \\ &= \|\mathbf{h}_n - \gamma \mathbf{P} \text{sgn}(\mathbf{x}_n)\|_2^2 \\ &= \|\mathbf{h}_n\|_2^2 - 2\gamma \mathbf{h}_n^T \mathbf{P} \text{sgn}(\mathbf{x}_n) + \gamma^2 \|\mathbf{P} \text{sgn}(\mathbf{x}_n)\|_2^2. \end{aligned} \quad (47)$$

According to (11),

$$\mathbf{h}_n^T \mathbf{A}^T = (\mathbf{x}_n - \mathbf{x}^*)^T \mathbf{A}^T = 0.$$

Considering

$$\begin{aligned} \mathbf{h}_n^T \mathbf{P} &= \mathbf{h}_n^T - \mathbf{h}_n^T \mathbf{A}^T (\mathbf{A} \mathbf{A}^T)^{-1} \mathbf{A} = \mathbf{h}_n^T, \\ (\mathbf{x}^*)^T \text{sgn}(\mathbf{x}_n) &\leq (\mathbf{x}^*)^T \text{sgn}(\mathbf{x}^*) = \|\mathbf{x}^*\|_1 \end{aligned}$$

and using Lemma 1, one can shrink the second item of (47) to

$$\mathbf{h}_n^T \text{sgn}(\mathbf{x}_n) \geq \|\mathbf{x}_n\|_1 - \|\mathbf{x}^*\|_1 \geq t \|\mathbf{h}_n\|_2. \quad (48)$$

Using (48) and (47), one has

$$\|\mathbf{h}_{n+1}\|_2^2 \leq \|\mathbf{h}_n\|_2^2 - 2\gamma t \|\mathbf{h}_n\|_2 + \gamma^2 \|\mathbf{P} \text{sgn}(\mathbf{x}_n)\|_2^2.$$

Consequently, for any $\mu > 1$, if

$$\|\mathbf{h}_n\|_2 \geq K\gamma = \frac{\mu}{2t} \max_{\mathbf{x} \in \mathbb{R}^N} \|\mathbf{P} \text{sgn}(\mathbf{x})\|_2^2,$$

one has

$$\begin{aligned} \|\mathbf{h}_{n+1}\|_2^2 &\leq \|\mathbf{h}_n\|_2^2 - d\gamma^2 \\ &= \|\mathbf{h}_n\|_2^2 - \gamma^2(\mu - 1) \max_{\mathbf{x} \in \mathbb{R}^N} \|\mathbf{P} \text{sgn}(\mathbf{x})\|_2^2. \end{aligned}$$

Theorem 4 is proved. \blacksquare

C. The Proof of Theorem 5

Proof: Noticing that \mathbf{u} is in the kernel of \mathbf{A} and \mathbf{P} is a symmetric projection matrix to the solution space, with (10) and (42), one has

$$\mathbf{P}\mathbf{u} = \mathbf{u}.$$

Because \mathbf{u} is a unit vector, it can be further derived that

$$\begin{aligned} \mathbf{u}^T \text{sgn}(\mathbf{x}) &= (\mathbf{P}\mathbf{u})^T \text{sgn}(\mathbf{x}) \\ &= \langle \mathbf{u}, \mathbf{P} \text{sgn}(\mathbf{x}) \rangle \\ &\leq \left\langle \frac{\mathbf{P} \text{sgn}(\mathbf{x})}{\|\mathbf{P} \text{sgn}(\mathbf{x})\|_2}, \mathbf{P} \text{sgn}(\mathbf{x}) \right\rangle \\ &= \|\mathbf{P} \text{sgn}(\mathbf{x})\|_2. \end{aligned} \quad (49)$$

Consider the definition of t in (12) and (45),

$$t \leq \inf_{\mathbf{x} \in \mathcal{X}_1 \cup \mathcal{X}_2} g(\mathbf{x}) \leq \inf_{\mathbf{x} \in \mathcal{X}_2} g(\mathbf{x}) \leq \mathbf{u}^T \text{sgn}(\mathbf{x}), \quad (50)$$

where \mathcal{X}_1 and \mathcal{X}_2 are defined in (39). Combining (49) and (50), consequently, the left inequality of (20) is proved.

Now let's turn to the right inequality of (20). Because of the property of projection matrix, $\mathbf{P} = \mathbf{P}^2$, the eigenvalue of \mathbf{P} is either 0 or 1. For all \mathbf{x} , one has

$$\begin{aligned} \|\mathbf{P} \text{sgn}(\mathbf{x})\|_2^2 &= \text{sgn}^T(\mathbf{x}) \mathbf{P} \text{sgn}(\mathbf{x}) \\ &\leq \max\{\lambda_{\mathbf{P}}\} \text{sgn}^T(\mathbf{x}) \text{sgn}(\mathbf{x}) \\ &= \|\text{sgn}(\mathbf{x})\|_2^2 \leq N, \end{aligned}$$

where $\{\lambda_{\mathbf{P}}\}$ denotes the eigenvalue set of \mathbf{P} . The arbitrariness of \mathbf{x} leads to

$$\max_{\mathbf{x} \in \mathbb{R}^N} \|\mathbf{P} \text{sgn}(\mathbf{x})\|_2 \leq \sqrt{N}.$$

Therefore, Theorem 5 is proved. \blacksquare

D. The Proof of Lemma 2

Proof: For K_{\min} satisfying (26), there exists $\mu' > 1$ such that

$$K_{\min} = \frac{\mu'}{2t} \max_{\mathbf{x} \in \mathbb{R}^N} \|\mathbf{P} \text{sgn}(\mathbf{x})\|_2^2. \quad (51)$$

Considering the recursion of sequence $\{\mathbf{x}'_n\}$ in (25), it is expected to prove that

$$\begin{aligned} \|\mathbf{x}'_n - \mathbf{x}^*\|_2^2 - 2\gamma t \|\mathbf{x}'_n - \mathbf{x}^*\|_2 + \gamma^2 \max_{\mathbf{x} \in \mathbb{R}^N} \|\mathbf{P} \text{sgn}(\mathbf{x})\|_2^2 \\ < (\|\mathbf{x}'_n - \mathbf{x}^*\|_2 - \gamma t (1 - 1/\mu'))^2, \end{aligned} \quad (52)$$

when

$$\|\mathbf{x}'_n - \mathbf{x}^*\|_2 \geq \gamma \cdot \frac{\mu'}{2t} \max_{\mathbf{x} \in \mathbb{R}^N} \|\mathbf{P} \text{sgn}(\mathbf{x})\|_2^2. \quad (53)$$

Using (53), the difference between the left side and the right side of (52) is

$$\begin{aligned} &\gamma^2 \left[\max_{\mathbf{x} \in \mathbb{R}^N} \|\mathbf{P} \text{sgn}(\mathbf{x})\|_2^2 - t^2 (1 - 1/\mu')^2 \right] \\ &- 2\gamma t \|\mathbf{x}'_n - \mathbf{x}^*\|_2 / \mu' \leq -\gamma^2 t^2 (1 - 1/\mu')^2 < 0. \end{aligned} \quad (54)$$

\blacksquare As a consequence, (52) holds and it leads to

$$\|\mathbf{x}'_{n+1} - \mathbf{x}^*\|_2 < \|\mathbf{x}'_n - \mathbf{x}^*\|_2 - \gamma t (1 - 1/\mu'). \quad (55)$$

According to (55), the quantity of decrease by each step is at least $\gamma t (1 - 1/\mu')$.

Considering that $\{\mathbf{x}_n\}$ has a faster convergence rate than that of $\{\mathbf{x}'_n\}$, and the trip of $\{\mathbf{x}_n\}$ is from $(K_{\max}\gamma)$ -ball to $(K_{\min}\gamma)$ -ball, consequently the iteration number is at most

$$\frac{(K_{\max} - K_{\min})\gamma}{\gamma t (1 - 1/\mu')} = \frac{2(K_{\max} - K_{\min})}{2t - \max_{\mathbf{x} \in \mathbb{R}^N} \|\mathbf{P} \text{sgn}(\mathbf{x})\|_2^2 / K_{\min}}.$$

\blacksquare

E. The Proof of Theorem 6

Proof: According to Lemma 2, the iteration number needed from $((n+1)K_0\gamma)$ -neighborhood to $(nK_0\gamma)$ -neighborhood is at most

$$\frac{K_0}{t - \max_{\mathbf{x} \in \mathbb{R}^N} \|\mathbf{P} \text{sgn}(\mathbf{x})\|_2^2 / (2nK_0)} = \frac{K_0}{t} \left(1 + \frac{1}{\mu_0 n - 1} \right), \quad (56)$$

where

$$K_0 = \frac{\mu_0}{2t} \max_{\mathbf{x} \in \mathbb{R}^N} \|\mathbf{P} \text{sgn}(\mathbf{x})\|_2^2$$

and μ_0 is larger than 1.

Assume that $M_0 = \|\mathbf{x}_0 - \mathbf{x}^*\|_2$ obeys

$$mK_0\gamma < M_0 \leq (m+1)K_0\gamma,$$

where m is a positive integer. Utilizing (56), the total iteration number from M_0 -neighborhood to $(K_0\gamma)$ -neighborhood is at most

$$\frac{K_0}{t} \sum_{n=1}^m \left(1 + \frac{1}{\mu_0 n - 1}\right), \quad (57)$$

which is less than

$$\frac{M_0}{t\gamma} + \frac{K_0}{t} \ln \left(\frac{M_0}{K_0\gamma} \right) + \frac{2K_0}{2t - \max_{\mathbf{x} \in \mathbb{R}^N} \|\mathbf{P} \text{sgn}(\mathbf{x})\|_2^2 / K_0}. \quad (58)$$

Thus Theorem 6 is proved. The relation between (57) and (58) comes from the following plain algebra,

$$\begin{aligned} (57) &< \frac{K_0}{t} \left[m + \frac{1}{\mu_0 - 1} + \sum_{n=2}^m \frac{1}{\mu_0(n-1)} \right] \\ &< \frac{K_0}{t} \left[m + \frac{1}{\mu_0 - 1} + \frac{1}{\mu_0} (\ln(m-1) + 1) \right] \\ &= \frac{K_0}{t} \left[m + \frac{1}{\mu_0} \ln(m-1) + \left(\frac{1}{\mu_0 - 1} + \frac{1}{\mu_0} \right) \right] \\ &< \frac{M_0}{t\gamma} + \frac{K_0}{t} \ln \left(\frac{M_0}{K_0\gamma} \right) + \frac{K_0}{t} \frac{\mu_0}{\mu_0 - 1} = (58). \end{aligned}$$

■

F. The Proof of Theorem 7

Proof: Similar to (47), by defining $\mathbf{h}'_n = \mathbf{x}_n - \mathbf{x}^*$ and $\mathbf{e}_n = \mathbf{A}(\mathbf{x}_n - \mathbf{x}^*)$, the deviation iterates by

$$\begin{aligned} \|\mathbf{h}'_{n+1}\|_2^2 &= \|\mathbf{h}'_n\|_2^2 - 2\gamma \mathbf{h}'_n{}^T \text{sgn}(\mathbf{x}_n) \\ &\quad + 2\gamma \mathbf{e}_n{}^T (\mathbf{A}\mathbf{A}^T)^{-1} \mathbf{A} \text{sgn}(\mathbf{x}_n) \\ &\quad + \gamma^2 \|\mathbf{P} \text{sgn}(\mathbf{x}_n)\|_2^2. \end{aligned} \quad (59)$$

From Lemma 3 and referring to (48), one has

$$\mathbf{h}'_n{}^T \text{sgn}(\mathbf{x}_n) \geq t \|\mathbf{h}'_n\|_2. \quad (60)$$

Next the third item of (59) will be studied. By the property of symmetric matrices,

$$\begin{aligned} &\|\mathbf{e}_n{}^T (\mathbf{A}\mathbf{A}^T)^{-1} \mathbf{A} \text{sgn}(\mathbf{x}_n)\|_2^2 \\ &= \text{sgn}^T(\mathbf{x}_n) \mathbf{A}^T (\mathbf{A}\mathbf{A}^T)^{-1} \mathbf{e}_n \mathbf{e}_n{}^T (\mathbf{A}\mathbf{A}^T)^{-1} \mathbf{A} \text{sgn}(\mathbf{x}_n) \\ &= \text{sgn}^T(\mathbf{x}_n) \mathbf{B} \text{sgn}(\mathbf{x}_n) \\ &\leq \max\{\lambda_{\mathbf{B}}\} \text{sgn}^T(\mathbf{x}_n) \text{sgn}(\mathbf{x}_n) \leq N \max\{\lambda_{\mathbf{B}}\}, \end{aligned} \quad (61)$$

where

$$\mathbf{B} = \mathbf{A}^T (\mathbf{A}\mathbf{A}^T)^{-1} \mathbf{e}_n \mathbf{e}_n{}^T (\mathbf{A}\mathbf{A}^T)^{-1} \mathbf{A}$$

and $\{\lambda_{\mathbf{B}}\}$ denote its eigenvalues. Notice that $\mathbf{e}_n{}^T (\mathbf{A}\mathbf{A}^T)^{-1} \mathbf{A} \in \mathbb{R}^{1 \times N}$, therefore $\text{rank}(\mathbf{B})$ is at most one, and at least $N - 1$

of the eigenvalues are zeros. Consequently, one has

$$\begin{aligned} \max\{\lambda_{\mathbf{B}}\} &= \text{tr}(\mathbf{B}) = \text{tr} \left(\mathbf{e}_n{}^T (\mathbf{A}\mathbf{A}^T)^{-1} \mathbf{A} \mathbf{A}^T (\mathbf{A}\mathbf{A}^T)^{-1} \mathbf{e}_n \right) \\ &= \mathbf{e}_n{}^T (\mathbf{A}\mathbf{A}^T)^{-1} \mathbf{e}_n \\ &\leq \max\{\lambda_{(\mathbf{A}\mathbf{A}^T)^{-1}}\} \mathbf{e}_n{}^T \mathbf{e}_n \leq 4\varepsilon^2 \lambda, \end{aligned} \quad (62)$$

where the last step can be derived by

$$\begin{aligned} \|\mathbf{e}_n\|_2 &= \|(\mathbf{y} - \mathbf{A}\mathbf{x}_n) - (\mathbf{y} - \mathbf{A}\mathbf{x}^*)\|_2 \\ &\leq \|\mathbf{y} - \mathbf{A}\mathbf{x}_n\|_2 + \|\mathbf{y} - \mathbf{A}\mathbf{x}^*\|_2 \leq 2\varepsilon. \end{aligned} \quad (63)$$

It can be easily seen that $\max\{\lambda_{(\mathbf{A}\mathbf{A}^T)^{-1}}\}$ is positive, if $\mathbf{A}\mathbf{A}^T$ is an invertible matrix.

Because $\mathbf{e}_n{}^T (\mathbf{A}\mathbf{A}^T)^{-1} \mathbf{A} \text{sgn}(\mathbf{x}_n)$ is a scalar, combining (61) and (62), one has

$$|\mathbf{e}_n{}^T (\mathbf{A}\mathbf{A}^T)^{-1} \mathbf{A} \text{sgn}(\mathbf{x}_n)| \leq 2\varepsilon \sqrt{N\lambda}. \quad (64)$$

For $\forall \mu > 1$, if

$$\|\mathbf{x}_n - \mathbf{x}^*\|_2 \geq \gamma \cdot \frac{\mu}{2t} \max_{\mathbf{x} \in \mathbb{R}^N} \|\mathbf{P} \text{sgn}(\mathbf{x})\|_2^2 + \varepsilon \cdot \frac{2}{t} \sqrt{N\lambda}, \quad (65)$$

using (60), (64) and (65), we have

$$\begin{aligned} &2(\mathbf{x}_n - \mathbf{x}^*)^T \text{sgn}(\mathbf{x}_n) - 2\mathbf{e}_n{}^T (\mathbf{A}\mathbf{A}^T)^{-1} \mathbf{A} \text{sgn}(\mathbf{x}_n) \\ &\geq \gamma \mu \max_{\mathbf{x} \in \mathbb{R}^N} \|\mathbf{P} \text{sgn}(\mathbf{x})\|_2^2. \end{aligned} \quad (66)$$

Combining (59) and (66), it can be concluded that under the condition of (65),

$$\|\mathbf{x}_{n+1} - \mathbf{x}^*\|_2^2 \leq \|\mathbf{x}_n - \mathbf{x}^*\|_2^2 - \gamma^2(\mu - 1) \max_{\mathbf{x} \in \mathbb{R}^N} \|\mathbf{P} \text{sgn}(\mathbf{x})\|_2^2.$$

Then Theorem 7 is proved. ■

ACKNOWLEDGEMENT

The authors wish to thank Jian Jin and three anonymous reviewers for their helpful comments to improve the quality of this paper.

REFERENCES

- [1] E. J. Candes, "Compressive sampling," *Proc. Int. Congr. Math.*, Madrid, Spain, 2006, vol. 3, pp. 1433-1452.
- [2] D. L. Donoho, "Compressed sensing," *IEEE Trans. Inf. Theory*, vol. 52, no. 4, pp. 1289-1306, Apr. 2006.
- [3] G. Valenzise, G. Prandi, M. Tagliasacchi, and A. Sarti, "Identification of sparse audio tampering using distributed source coding and compressive sensing techniques," *Journal on Image and Video Processing*, vol. 2009, Jan. 2009.
- [4] M. Lustig, D. L. Donoho, and J. M. Pauly, "Sparse MRI: The application of compressed sensing for rapid MR imaging," *Magnetic Resonance in Medicine*, vol. 58, no. 6, pp. 1182-1195, Dec. 2007.
- [5] J. Wright, Y. Ma, J. Mairal, G. Sapiro, T. S. Huang, and S. Yan, "Sparse representation for computer vision and pattern recognition," *Proceedings of the IEEE*, vol. 98, no. 6, pp. 1031-1044, June 2010.
- [6] W. U. Bajwa, J. Haupt, A. M. Sayeed, and R. Nowak, "Compressive wireless sensing," *Proc. 5th Intl. Conf. on Information Processing in Sensor Networks (IPSN'06)*, Nashville, TN, 2006, pp. 134-142.
- [7] Y. C. Pati, R. Rezaifar, and P. S. Krishnaprasad, "Orthogonal matching pursuit: Recursive function approximation with applications to wavelet decomposition," *Proc. 27th Annu. Asilomar Conf. Signals, Syst., Comput.*, Pacific Grove, CA, Nov. 1993, vol. 1, pp. 40-44.
- [8] J. Tropp and A. Gilbert, "Signal recovery from random measurements via orthogonal matching pursuit," *IEEE Trans. Inf. Theory*, vol. 53, no. 12, pp. 4655-4666, Dec. 2007.
- [9] M. A. Davenport and M. B. Wakin, "Analysis of orthogonal matching pursuit using the restricted isometry property," *IEEE Trans. Inf. Theory*, vol. 56, no. 9, pp. 4395-4401, Sept. 2010.

- [10] D. L. Donoho, Y. Tsaig, and J. L. Starck, "Sparse solution of under-determined linear equations by stagewise orthogonal matching pursuit," 2007, submitted for publication.
- [11] D. Needell and R. Vershynin, "Uniform uncertainty principle and signal recovery via regularized orthogonal matching pursuit," *Foundations of Computational Mathematics*, vol. 9, no. 3, pp. 317-334, 2009.
- [12] D. Needell and R. Vershynin, "Signal recovery from incomplete and inaccurate measurements via regularized orthogonal matching pursuit," *IEEE J. Sel. Topics Signal Process.*, vol. 4, no. 2, pp. 310-316, Apr. 2010.
- [13] D. Needell and J. A. Tropp, "CoSaMP: Iterative signal recovery from incomplete and inaccurate samples," *Appl. Comput. Harmonic Anal.*, vol. 26, no. 3, pp. 301-321, 2009.
- [14] W. Dai and O. Milenkovic, "Subspace pursuit for compressive sensing: Closing the gap between performance and complexity," *IEEE Trans. Inf. Theory*, vol. 55, no. 5, pp. 2230-2249, May 2009.
- [15] T. Blumensath and M. E. Davies, "Iterative hard thresholding for compressed sensing," *Appl. Comput. Harmonic Anal.*, vol. 27, no. 3, pp. 265-274, Nov. 2009.
- [16] M. Saunders, "PDCO: Primal-dual interior method for convex objectives," 2002 [Online]. Available: <http://www.stanford.edu/group/SOL/software/pdco.html>.
- [17] C. Paige and M. Saunders, "LSQR: An algorithm for sparse linear equations and sparse least squares," *ACM Trans. Math. Software*, vol. 8, no. 1, pp. 43-71, 1982.
- [18] S. Kim, K. Koh, M. Lustig, S. Boyd, and D. Gorinvesky, "An interior-point method for large-scale ℓ_1 -regularized least squares," *IEEE J. Sel. Topics Signal Process.*, vol. 1, no. 4, pp. 606-617, Dec. 2007.
- [19] B. Efron, T. Hastie, I. Johnstone, and R. Tibshirani, "Least angle regression," *Ann. Statist.*, vol. 32, no. 2, pp. 407-499, 2004.
- [20] M. A. T. Figueiredo, R. D. Nowak, and S. J. Wright, "Gradient projection for sparse reconstruction: Application to compressed sensing and other inverse problems," *IEEE J. Sel. Topics Signal Process.*, vol. 1, no. 4, pp. 586-597, Dec. 2007.
- [21] S. Wright, R. Nowak, and M. Figueiredo, "Sparse reconstruction by separable approximation," *IEEE Trans. Signal Process.*, vol. 57, no. 7, pp. 2479-2493, July 2009.
- [22] E. van den Berg, M. P. Friedlander, "Probing the Pareto frontier for basis pursuit solutions," *SIAM J. Sci. Comput.*, vol. 31, pp. 890-912, 2008.
- [23] S. Becker, J. Bobin, and E. Candes, "NESTA: A fast and accurate firstorder method for sparse recovery," *SIAM J. Imag. Anal.*, vol. 4, pp. 1-39, 2011.
- [24] M. V. Afonso, J. M. Bioucas-Dias, M. A. T. Figueiredo, "A fast algorithm for the constrained formulation of compressive image reconstruction and other linear inverse problems," *ICASSP 2010*, pp. 4034-4037, Mar. 2010.
- [25] I. F. Gorodnitsky, J. George, and B. D. Rao, "Neuromagnetic source imaging with FOCUSS: A recursive weighted minimum norm algorithm," *Electroencephalography and Clinical Neurophysiology*, pp. 231-251, 1995.
- [26] C. Rich and W. Yin, "Iteratively reweighted algorithms for compressive sensing," *ICASSP 2008*, pp. 3869-3872, Apr. 2008.
- [27] J. Portilla, "Image restoration through l0 analysis-based sparse optimization in tight frames," *Proc. IEEE Int. conf. Image Process.*, pp. 3909-3912, Nov. 2009.
- [28] J. Jin, Y. Gu, and S. Mei, "A Stochastic gradient approach on compressive sensing signal reconstruction based on adaptive filtering framework," *IEEE J. Sel. Topics Signal Process.*, vol. 4, no. 2, Apr. 2010.
- [29] E. J. Candes and T. Tao, "Decoding by linear programming," *IEEE Trans. Inf. Theory*, vol. 51, no. 12, Dec. 2005.
- [30] E. J. Candes, "The restricted isometry property and its implications for compressed sensing," *Comptes Rendus Mathematique*, Series I, vol. 346, no. 9-10, pp. 589-592, May 2008.
- [31] B. Bah and J. Tanner, "Improved bounds on restricted isometry constants for Gaussian matrices," *arXiv:1003.3299v2*, 2010.
- [32] J. D. Blanchard, C. Cartis, and J. Tanner, "Compressed sensing: How sharp is the restricted isometry property," *arXiv:1004.5026v1*, 2010.
- [33] E. J. Candes and J. Romberg, "Sparsity and incoherence in compressive sampling," *Inverse Problems*, vol. 23, no. 3, pp. 969-985, 2007.
- [34] E. J. Candes, J. Romberg, and T. Tao, "Stable signal recovery from incomplete and inaccurate measurements," *Communications on Pure and Applied Mathematics*, vol. 59, no. 8, pp. 1207-1223, Aug. 2006.
- [35] Z. Ben-Haim, Y. C. Eldar, and M. Elad, "Coherence-based performance guarantees for estimating a sparse vector under random noise," *IEEE Trans. Signal Process.*, vol. 58, no. 10, pp. 5030-5043, Oct. 2010.